Title

Inhibition of soluble epoxide hydrolase in mice promotes reverse cholesterol transport and regression of atherosclerosis

Authors

Shen, Li

Peng, Hongchun

Peng, Ran

et al.

Peer reviewed

Inhibition of soluble epoxide hydrolase in mice promotes reverse cholesterol transport and regression of atherosclerosis

Li Shen[a], **Hongchun Peng**[b], **Ran Peng**[a], **Qingsong Fan**[c], **Shuiping Zhao**[a], **Danyan Xu**[a,*], **Christophe Morisseau**[d], **Nipavan Chiamvimonvat**[e], and **Bruce D. Hammock**[d]

[a] Department of Cardiology, Internal Medicine, Xiangya Second Hospital, Central South University, Changsha, 410011, PR China

[b] Department of Orthopaedics and Emergency, Changsha Central Hospital, Changsha, 410011, PR China

[c] Department of Pathology, Xiangya Second Hospital, Central South University, Changsha, Hunan Province, 410001, PR China

[d] Department of Entomology and Comprehensive Cancer Center, University of California, Davis, CA, 95616, USA

[e] Division of Cardiovascular Medicine, Department of Internal Medicine, University of California, Davis, CA, 95616, USA

Abstract

Adipose tissue is the body largest free cholesterol reservoir and abundantly expresses ATP binding cassette transporter A1 (ABCA1), which maintains plasma high-density lipoprotein (HDL) levels. HDLs have a protective role in atherosclerosis by mediating reverse cholesterol transport (RCT). Soluble epoxide hydrolase (sEH) is a cytosolic enzyme whose inhibition has various beneficial effects on cardiovascular disease. The sEH is highly expressed in adipocytes, and it converts epoxyeicosatrienoic acids (EETs) into less bioactive dihydroxyeicosatrienoic acids. We previously showed that increasing EETs levels with a sEH inhibitor (sEHI) (*t*-AUCB) resulted in elevated ABCA1 expression and promoted ABCA1-mediated cholesterol efflux from 3T3-L1 adipocytes. The present study investigates the impacts of *t*-AUCB in mice deficient for the low density lipoprotein (LDL) receptor (Ldlr$^{-/-}$ mice) with established atherosclerotic plaques. The sEH inhibitor delivered *in vivo* for 4 weeks decreased the activity of sEH in adipose tissue, enhanced ABCA1 expression and cholesterol efflux from adipose depots, and consequently increased HDL levels. Furthermore, *t*-AUCB enhanced RCT to the plasma, liver, bile and feces. It also showed the reduction of plasma LDL-C levels. Consistently, *t*-AUCB–treated mice showed reductions in the size of atherosclerotic plaques. These studies establish that raising adipose ABCA1 expression, cholesterol efflux, and plasma HDL levels with *t*-AUCB treatment promotes RCT, decreasing

* Corresponding author. xudanyan02@sina.com (D. Xu)..

LDL-C and atherosclerosis regression, suggesting that sEH inhibition may be a promising strategy to treat atherosclerotic vascular disease.

Keywords

ATP binding cassette transporter A1; Epoxyeicosatrienoic acids; Soluble epoxide hydrolase; High density lipoprotein; Reverse cholesterol transport

1. Introduction

Plasma high density lipoprotein cholesterol (HDL-C) levels bear a strong reverse relationship with atherosclerotic cardiovascular disease risk [1]. HDL plays a key role in reverse cholesterol transport (RCT) by promoting cholesterol efflux from peripheral cells, and delivering the cholesterol to the liver for excretion, a process that is believed to be atheroprotective [2]. Many studies strongly suggest that HDL-raising strategies may be effective therapy for the treatment of atherosclerosis [3–5]. However, our understanding of the mechanisms that contribute to HDL regulation remain largely incomplete. ATP-binding cassette transporter A1 (ABCA1) is an essential membrane protein for the initial step of HDL biogenesis by facilitating the efflux of cellular free cholesterol to extracellular lipid-free apolipoprotein A-I (apoA-I), forming nascent HDL particles [6]. The critical role of ABCA1 in HDL metabolism was first identified as the gene mutated in Tangier disease [7], which is characterized by markedly low levels of circulating HDL-C [6]. ABCA1 is highly expressed in several tissues [8]. The expression of ABCA1 in liver, adipose tissue and intestine are reported to contribute plasma HDL-C pool [9,10]. The liver is considered the principal organ for cholesterol biosynthesis and catabolism through bile acid production. However, in obese individuals, adipose tissues are the largest cholesterol reservoir [11]. Moreover, the obesity state is associated with lower plasma HDL-C, which may be attributable to the impaired ability of adipocytes to efflux cholesterol to HDL [1]. Thus, in obese persons, ABCA1 role in HDL regulation is more important in adipose tissue than in liver and intestine. In 2010, Zhang et al. [12] presented the first evidence that adipocytes transfer of cholesterol to HDL *in vitro* is mediated by ABCA1. Furthermore, Chung et al. [13] findings suggested a role for adipose ABCA1 in contributing to plasma HDL-C, particularly in the obese state. Lack of adipose ABCA1 impaired cholesterol efflux to apoA-I, and reduced circulating HDL-C. Therefore, promoting adipose ABCA1-mediated cholesterol efflux should raise HDL-C levels, and thus have positive effects on reducing atherosclerosis.

The expressions of ABCA1 in adipose tissue is upregulated in states of cholesterol excess by transcriptional and post-transcriptional mechanisms [14]. The enzyme soluble epoxide hydrolase (sEH), which metabolizes endogenous epoxyeicosatrienoic acid (EETs), is abundantly expressed in adipose tissue, and its expression and activity increase with obesity [15]. Recently, our group reported that inhibition of endogenous sEH in adipocytes by a sEH inhibitor (*t*-AUCB) results in an increase in ABCA1 mRNA and protein expression, indicating a possible relevant role for adipose sEH in regulating ABCA1 [16]. Separately, sEHI were found to reduce the progression of atherosclerotic disease in apoE $^{-/-}$ mice

[17,18]. These data suggest that inhibition of sEH may be an attractive therapeutic target for the treatment of cardiovascular disease; however, many questions remain to be addressed, in particular regarding the effect of sEH inhibition on the functionality of produced HDL and its ability to promote RCT.

In the current study, we tested the impact of sEH inhibition on RCT and atherosclerosis in the hypercholesterolemic and obese mouse model deficient for the LDL receptor (Ldlr$^{-/-}$ mice). Atherosclerosis was first established in Ldlr$^{-/-}$ mice by feeding them an atherogenic diet (ATD), after which they were treated with an sEHI (t-AUCB) for 4 weeks. We demonstrated herein that sEH expression is increased in the adipose tissue of mice fed ATD. Importantly, inhibition of sEH in mice effectively decreases plasma LDL-C levels, increases ABCA1 expression in adipose tissue and effectively raises circulating HDL. Furthermore, inhibition of sEH expression in adipose tissue effectively increases RCT and decreases the size of atherosclerotic plaque. These data establish that inhibition of endogenous sEH therapeutically reduces plasma LDL-C, increases ABCA1 expression in adipose tissue, raises plasma HDL, enhances RCT and induces regression of atherosclerosis.

2. Methods

2.1. Drug delivery

The potent and selective sEHI *trans*-4-[4-(3-adamantan-1-yl-ureido)-cyclohexyloxy]-benzoic acid (t-AUCB) was synthesized by Dr. Sung Hee Hwang from the laboratory of Pr. Bruce D Hammock [19]. The structure and physical properties are shown in online Data Supplement S1 and Fig. 1. For mice treatment, 0.5 mg t-AUCB was added to 1.0 mL PEG400 and ultrasonicated until the suspension became a completely clear liquid. The stock solution (500 mg/L) was diluted to concentrations of 50, 15 and 5 mg/L. Compared with earlier sEHI, such as AUDA, t-AUCB has improved water solubility and high oral availability such that can it be delivered in drinking water. The water solubility of t-AUCB is 160 mg/L.

2.2. Mice

Animal experiments were approved by the Institutional Animal Care and Use Committee of the Second Xiangya Hospital of Central South University, China. Forty-two 8-week-old male Ldlr$^{-/-}$ mice (C57BL/6 background) were weaned at 4 weeks of age and placed on an ATD that containing 21% fat and 0.15% cholesterol for 14 weeks, at which point mice were either sacrificed (baseline) (n = 4) or switched to standard chow diet (SCD) for 4 weeks. Coincident with the switch to SCD (n = 6), mice were randomized into 4 groups (n = 8): no treatment (vehicle only) and t-AUCB 5, 15 or 50 mg/L. The mice were observed to drink approximately 3–4 mL water per day, which was consistent with published studies [18], indicate this procedure gives a dose of approximately 0.5–5 mg t-AUCB per kg per day, clearly with high levels of intake at night. Each mouse was housed in a separate cage in order to monitor the daily water and drug intake.

2.3. Measurement of the concentrations of sEHI in the plasma

Mice were sacrificed after 4 weeks of treatment, and then the blood concentrations of *t*-AUCB were measured as the method, which has previously been described [20]. At the end of experiments, 10 μL of whole blood was placed into 50 μL distilled water containing 10 μL of propane 1, 2-diol and EDTA, and then mixed followed by addition of 200 μL of ethyl acetate. Similarly, added 50 μL internal standard and shook again. The extracted samples were analyzed by liquid chromatography coupled with mass spectrometry [18].

2.4. sEH activity assay

Measurement of sEH activity has previously been described [21,22]. Briefly, epididymal adipose tissue depots were homogenized in PMSF, and cytosolic supernatants were obtained by centrifugation. In brief, 100 μL of supernatants were incubated with or without 20 μM *t*-AUCB at 30 °C for 10 min in 96-well black assay plates, and 80 mM epoxy fluor 7 in 100 μL reaction buffer (50 mM Tris–HCl buffer containing 0.2 mg/mL BSA, pH 7.0) was added to each well. After incubation at 30 °C for 30 min, fluorescence was determined by use of a Spectra Fluor Plus Xuorescent plate reader (Tecan Systems, San Jose, CA, USA) with excitation wavelength 330 nm and 465 nm at 30 °C. sEH activity was the corrected sample fluorescence intensity calculated by sample fluorescence values for the sEHI subtracted from those of the non-sEHI.

2.5. Plasma cholesterol determination and fast protein liquid chromatography

Plasma was collected either by tail or retro-orbital plexus bleeding of mice fasted for 4 h. Plasma total cholesterol (TC), low density lipoprotein cholesterol (LDL-C) and HDL-C levels were measured by enzymatic method (bioMerieux, Lyon, France) using an automated analyzer (Type 7170A, Hitachi). For fast protein liquid chromatography analysis, 300 μL pooled plasma (n = 4 mice total) was separated on a Superose-6 TM column (Amersham Biosciences) at a flow rate of 0.4 mL/min as described previously [23].

2.6. Adipose cholesterol determination

Lipid extracts of liver tissue were assayed for cholesterol according to the manufacturer's protocol using the Cholesterol Quantification Kit (BioVision, Mountain View, CA). Data were normalized to tissue wet weight or protein, measured by the Lowry assay.

2.7. Cholesterol efflux from adipose tissue

To establish the *ex vivo* cultures of adipose tissue, freshly isolated epididymal fat (0.1–0.2 g) was minced into 2 mm pieces, moved into 10 cm cell culture dishes, and incubated overnight in 2.0 mL serum-free DMEM/F12 (Gibico). The next day, adipose tissue cultures were washed thoroughly with caution to remove floating cells without aspirating the minced tissue explants. Measurement of cholesterol efflux was conducted as described in previous studies [13]. Briefly, *ex vivo* cultures of adipose tissue were incubated with 5 μCi of ^{3}H-cholesterol for 24 h. Adipose tissue explants were then washed carefully, and 1 mL fresh serum-free medium was added. Cholesterol efflux was initiated by adding either 20 μg protein/mL of human apoA-I as acceptors. After 4 h of additional incubation, cholesterol efflux was quantified by measuring ^{3}H-cholesterol in medium and in the cells after 10%

NaOH extraction. Percentage efflux was calculated as follows: cpm ^{3}H-cholesterol in medium/cpm ^{3}H-cholesterol (medium + cells)$\times$ 100%.

2.8. Murine ex vivo cholesterol efflux

Plasma was collected either via tail vein or retro-orbital plexus after 48 h and 5% serum was used as a cholesterol efflux acceptor. *Ex vivo* efflux from labeled adipocytes to 5% serum or a minimal essential medium control was measured over a 4 h period.

2.9. In vivo RCT assay

Raw264.7 macrophages were maintained in 5% CO_2 at 37 °C in DMEM supplemented with 10% FBS. For RCT assays, macrophages were washed twice and incubated with 37.5 μg/mL acetylated LDL (acLDL) and 5 μCi/ml ^{3}H-cholesterol for 24 h as described previously [24]. On average, cell suspensions with 2.5 10^5 cells containing 1.15 10^6 cpm in 0.75 mL DMEM were injected intraperitoneally into individually housed mice treated with *t*-AUCB for 4 weeks as described above. Blood and bile acid was obtained after 48 h at sacrifice. Feces were also collected for 48 h after injection and homogenized in 50% NaOH overnight, after which an aliquot was used for liquid scintillation counting (LSC) to measure radioactivity. Liver samples were collected and incubated with hexane/isopropanol (3:2) for 48 h and then dried overnight. Lipids were resolubilized in liquid scintillation fluid, and radioactivity was counted. RCT to plasma, feces, and liver was calculated as a percentage of the total cpm injected.

2.10. Evaluation of atherosclerotic lesions

The mice were euthanized by exsanguination and then 4% paraformaldehyde perfusion-fixed via a cannula placed in the left ventricle of the heart. The arteries were removed from the ascending aorta to ileal bifurcation and placed in 4% paraformaldehyde overnight at room temperature. The intimal surface was opened longitudinally and stained with Sudan III. Stained aortas were pinned on the surface of black wax in a dissecting pan and images were captured using a Cannon digital camera. Image J software quantitated the areas of luminal atherosclerotic lesions. From the valves to aortic root ($\approx$420 μm), six slices were used to determine plaque area following hematoxylin and eosin staining (magnification 20$\times$).

2.11. Laboratory methods

A description of general laboratory methods including lipid and lipoprotein assays, quantitative real-time polymerase chain reaction and Western blot analysis is presented in the Methods in online Data Supplement S4.

2.12. Statistical analysis

Data are reported as the mean $\pm$ standard error. For atherosclerosis and cholesterol efflux analyses, all comparisons were made using a one-way ANOVA and $P < 0.05$ (two-sided) was considered as statistically significant.

3. Results

3.1. t-AUCB decreases expression of sEH in adipose tissue and increases targeted gene ABCA1 expression

To assess the effect of inhibiting sEH with *t*-AUCB in a model of established atherosclerosis, Ldlr$^{-/-}$ mice were first fed ATD for 14 weeks (baseline), after which they were switched to a SCD to block atherosclerosis progression and treated with 5, 15, 50 mg/L *t*-AUCB or untreated control (0 mg/L). To determine the efficacy of the treatment, the blood concentrations of *t*-AUCB were measured. Separate studies indicated that, when *t*-AUCB is administered in drinking water, its blood concentrations are approximately two fold higher at night than during the day due to increased nocturnal water consumption. In our study, blood samples were taken during the day 4 h after the lights were turned on. As expected, the plasma concentrations of *t*-AUCB increased in a dose dependent manner (plasma concentrations were under the quantitative limit in the control group ($n = 14$), while plasma concentrations were 35.7 ± 10.4 nM, 58.2 ± 26.6 nM and 113.2 ± 35.6 nM for the 5 mg/L (n m= 8), 15 mg/L (n = 8), and 50 mg/L ($n = 8$) treated mice, respectively). The daily water intake was about 3–4 mL per animal, and no significant differences were observed among different groups of mice.

We previously showed that sEHI could inhibit the activity of sEH in 3T3-L1 adipocytes and increase cellular EETs levels [16]. To gain insight into the expression among fat depots, we initially measured relative sEH expression by Western-blot in different fat depots of ATD mice. There was a significant variation in sEH expression among fat depots (epididymal > subcutaneous (inguinal) > pericardial > brown fat) (Fig. 1A). Next, we examined the effect of sEHI on sEH activity and expression in epididymal fat depots from mice. As compared with SCD group, ATD mice have 1.6-fold higher sEH activity, while for the *t*-AUCB treatment groups, sEH activity was largely inhibited in a dose-dependent manner (Fig. 1B). Consistently, levels of sEH protein, detected by Western Blot, were decreased in *t*-AUCB-treated mice compared with those of control mice (Fig. 1C, D). In adipocytes, sEHI treatment increases cellular ABCA1 expression via the EETs-ABCA1 pathway [16]. To determine whether increased EET levels also regulate adipose ABCA1 expression *in vivo*, we measured the expression levels of target genes ABCA1 in epididymal adipose tissue after 4 weeks of *t*-AUCB treatment. We observed that ABCA1 mRNA expression of the epididymal adipose tissue decreased in ATD mice compared to SCD groups, while its expression in the *t*-AUCB-treated groups was significantly increased compared with that of the untreated mice. However, no change in ABCG1 and SR-BI mRNA was observed (Fig. 2A). Furthermore, ABCA1 protein expression was dose-dependently increased in epididymal fat depot of *t*-AUCB-treated mice, compared with those of control groups, and no significant changes in ABCG1 and SR-BI protein expression (Fig. 2B, C). In addition, there were no significant changes of ABCA1, ABCG1 and SR-BI protein expression in liver (Fig. 2D). Together these data demonstrate that *t*-AUCB effectively inhibits sEH activity and selectively increases expression of ABCA1 in adipose tissue.

3.2. t-AUCB treatment increases HDL and enhances ABCA1-mediated cholesterol efflux ex vivo

Because increased ABCA1 expression in adipose tissue is predicted to augment HDL biogenesis [13], circulating HDL-C levels were measured. Ldlr$^{-/-}$ mice with ATD develop obese and severe hyperlipidemia that increased levels of total cholesterol (TC), LDL-C and reduced levels of HDL-C (Table 1). Treatment of Ldlr$^{-/-}$ mice with t-AUCB for 4 weeks raised HDL-C levels in a dose-dependent manner compared with that of the control mice (Table 1). Furthermore, LDL-C levels were reduced compared with the control group, which is consistent with previous work [16] (Table 1). There was no difference in plasma triglyceride and TC among mice that were treated with t-AUCB or control groups (Table 1). Analysis of lipoproteins by FPLC showed an increase in cholesterol content of the HDL fractions (fractions 59–75) of the t-AUCB-treated mice compared with those non-treated controls, but minimal effect on LDL and VLDL cholesterol mass (Fig. 3A). To determine whether increase of ABCA1 in adipose tissue resulted in decreased cholesterol content due to cholesterol efflux, cholesterol contents of epididymal fat from 3 to 4 mice after 4 weeks of t-AUCB treatment were measured. There is a dose-related decrease in cholesterol content in epididymal fat that reached statistical significance in t-AUCB treated mice (Fig. 3B). Furthermore, freshly isolated epididymal fat from t-AUCB-treated mice were minced into small pieces and cultured in cell dishes with DMEM/F12. Then we incubated with ^{3}H-cholesterol for 24 h, washed thoroughly with caution to remove floating cells without aspirating the minced tissue explants, and incubated them for 4 h with apoA-I to measure ABCA1-dependent cholesterol efflux. ABCA1-dependent ^{3}H-cholesterol efflux to apoA-I was highly elevated in t-AUCB treated epididymal fat compared with control groups (Fig. 3C). More importantly, cholesterol efflux from mouse plasma-mediated adipocytes was examined in vitro. In our preliminary study, we observed that cholesterol efflux increased linearly with plasma concentration, up to a concentration of 0.6% in the media. At higher plasma concentrations, there appeared to be saturation of the adipocytes machinery that mediates efflux. We therefore used a 0.5% concentration of plasma for all subsequent experiments. We demonstrated that t-AUCB treatment dose-dependently increased the counts of plasma ^{3}H-cholesterol from (5.04 ± 0.48)% in cells exposed to plasma of no t-AUCB control mice to 8.19 ± 2.12%, 12.00 ± 1.36% and 12.18 ± 0.72% in cells exposed to plasma of mice treated with t-AUCB at 5, 15 or 50 mg/L, respectively (all $P < 0.05$) (Fig. 3D). It was consistent with our previous study that t-AUCB promotes excess cholesterol efflux from adipocyte and increases the expression of ABCA1 [16]. These results suggested that increased cholesterol efflux from adipose explants or 3T3-L1 adipocyte were possibly due to activate the expression of functional ABCA1.

3.3. t-AUCB treatment enhances RCT in vivo

To determine whether higher HDL levels in response to t-AUCB treatment upregulates cholesterol transport from peripheral cells to the liver for further excretion into bile and feces, we performed an in vivo RCT assay that traces ^{3}H-cholesterol from macrophages loaded with cholesterol ex vivo.

t-AUCB-treated mice injected intraperitoneally with ^{3}H-cholesterol-labeled Raw264.7 macrophages showed much higher plasma ^{3}H-counts ($P < 0.05$), exhibiting an 81–197%

increase in a concentration dependent manner compared with the *t*-AUCB 0 mg/L group (Fig. 4A). We further assessed the effects of *t*-AUCB on subsequent steps in the RCT pathway involving hepatic ^{3}H-cholesterol flux through the liver to bile and feces. Liver ^{3}H-levels in *t*-AUCB treated mice showed dose dependent increases of 5%, 19% and 62.3%, and the ^{3}H-level in 50 mg/L *t*-AUCB treated mice was greater than that in the 0 mg/L *t*-AUCB group. The most pronounced effect of *t*-AUCB to the RCT step was on ^{3}H-cholesterol secretion from the liver to bile and feces. ^{3}H-levels in the bile acids were significantly increased in *t*-AUCB treated mice in a dose dependent manner (5 mg/L by 155%, 15 mg/L by 178% and 50 mg/L by 233%) compared with the 0 mg/L *t*-AUCB group (all $P < 0.05$) (Fig. 4B). Furthermore, *t*-AUCB treated mice exhibited higher fecal ^{3}H-cholesterol levels than the 0 mg/L *t*-AUCB mice ($P < 0.05$) (Fig. 4B) and *t*-AUCB increased fecal total sterol excretion to a similar extent (65–226%) compared with ^{3}H-cholesterol levels in bile acids. Together, these results establish that *t*-AUCB not only increases circulating HDL, but enhances the RCT pathway by which excess cholesterol is removed from peripheral tissues, a process that is particularly important in the removal of cholesterol from atherosclerotic lesions.

3.4. t-AUCB treatment induces atherosclerosis regression

Data from mouse models of apoA-I overexpression or HDL infusion suggest that raising HDL-C favorably attenuates atherosclerosis [25]. We, thus, hypothesized that the enhanced RCT in *t*-AUCB-treated mice would promote removal of cholesterol from vessel wall foam cells, leading to plaque regression. The mean lesion area of Ldlr$^{-/-}$ mice were almost completely covered with atherosclerotic lesions in the aortic arches, descending thoracic and abdominal aortas after 14 weeks of ATD feeding (baseline). By contrast, striking decrease in the extent of aortic atherosclerosis were observed in visualized (unstained) plaque among 5, 15 and 50 mg/L *t*-AUCB treated mice compared with the no *t*-AUCB animals (Fig. 5A). Likewise, sudan III staining of atherosclerotic lesions of aorta *en face* similarly showed significant reductions of lesion size (Fig. 5B). Examination of hematoxylin- and eosin-stained cross sections of the aortic root showed that in addition to a reduction in size, plaques in *t*-AUCB-treated mice appeared to have been substantially remodeled compared with plaques in control mice (Fig. 4C). Furthermore, quantization of the percentage area covered by atherosclerotic lesions using Photoshop CS 9.0 showed that *t*-AUCB treatment had a dose dependent effect on reducing aortic plaque formation (Fig. 5D, E).

4. Discussion

Although our previous reports showed that sEH inhibition increases ABCA1 expression and cholesterol efflux in 3T3-L1 adipocytes [16], the current innovative study demonstrates that in Ldlr$^{-/-}$ mice the sEHI *t*-AUCB penetrates the adipose tissue of the mice and inhibits sEH activity and expression. This increases the levels of epoxy-fatty acids such as EETs from arachidonic acid, which upregulate ABCA1 expression and enhance cholesterol removal. Building on previous reports showing that inhibition sEH in apoE knockout mice attenuated the development of atherosclerosis [17,18], our study shows that inhibition of sEH in Ldlr$^{-/-}$ mice reduces plasma LDL-C, raises circulating HDL, enhances RCT, and promotes the regression of established atherosclerosis. However, the mechanism is still unclear. This

study demonstrated that increased adipose ABCA1 and circulating HDL-C levels caused by *t*-AUCB treatment promote removal of excess cholesterol from the periphery into the RCT pathway for excretion. The reduction of LDLC and increase in RCT is very likely responsible for the favorable effect of *t*-AUCB on atherosclerosis in that we observed reductions in lesion area. Together, these data establish sEH as an attractive therapeutic target for regressing atherosclerosis.

EETs are synthesized from intracellular arachidonic acid by cytochrome P450s [26]. EETs and other epoxy-fatty acids possess a wide array of potent biological actions in regulating lipid metabolism and treating obesity and insulin resistance [27,28]. The sEH plays a key role in regulating the levels of EETs by effectively degrading them into more polar and usually less potent metabolites, dihydroxyeicosatrienoic acids (DHETs) [29]. sEH activity is increased in epididymal fat pads of mice fed a high fat diet [15]. Moreover, the increased sEH expression in obese rodents can be directly attributed to obesity and adipose endoplasmic reticulum stress [30]. The sEHI targeting adipose tissue could inhibit the sEH activity and protein expression [30]. The current findings are in line with a previous study that reported increased adipose sEH activity in mice fed an ATD for 14 weeks [30]. However, another study indicates that high fat feeding (for 20 weeks) does not alter adipose sEH expression (but elevates adipose sEH activity) [15]. The discrepancy in adipose sEH protein expression could be due to differences in diets (42% kcal from fat versus 20% fat used in this study) and/or duration of the challenge.

ABCA1 modulates the rate-limiting step in the biogenesis of HDL particles by mediating the efflux of cellular cholesterol to apoA-I and therefore plays a critical role in RCT [31]. Liver and intestine ABCA1 expression are the mainly sites that affect plasma HDL formation [9,10]. In addition to the additive contribution of hepatic and intestinal ABCA1 to the HDL-C pool, conditional deletion of ABCA1 in the brain also surprisingly reduced HDL-C [32]. Recently, much evidence has pointed toward a potential contribution of adipose in mediating HDL lipidation. Adipose tissue is the major storage place for cholesterol within the body [33], and therefore represents a large pool of substrate to support HDL biogenesis. Adipose tissue expresses high levels of the key cholesterol transporter ABCA1, providing a gateway for cholesterol to efflux onto HDL [12]. Adipocytes promote HDL lipidation *in vivo*, and the absence of adipocyte ABCA1 expression impairs this process [12]. Chung et al. [13] recently reported that specific deletion of adipose ABCA1 significantly reduces plasma HDL-C. These data suggest that adipose ABCA1 regulates circulating HDL-C *in vivo*.

Our previous study demonstrated that the inhibition of endogenous sEH by *t*-AUCB elevated ABCA1 expression in 3T3L1 adipocytes [16]. We consistently observed that *t*-AUCB increased the expression of ABCA1 in adipose tissue and no significant change in ABCG1 and SR-BI expression. In addition, *t*-AUCB has no influence on hepatic ABCA1, ABCG1 and SR-BI expression. ABCA1 is important regulator of cholesterol efflux from adipocytes [12,13]. *t*-AUCB promoted apoA-I-induced cholesterol efflux in adipocytes by increasing ABCA1 expression [16]. Furthermore, apoA-I mediated cholesterol efflux from epididymal adipose explants was highly elevated in the increase of functional ABCA1 expression. Consistently, plasma from *t*-AUCB treated mice also promoted adipocyte cholesterol efflux *in vitro*. Interesting, adipose depots differentially contribute to cholesterol

efflux. The highest contribution is from epididymal depots [1,13]. Consistently, depot-specific differences in adipose sEH expression was observed, with higher expression in metabolically active epididymal depots compared with the less metabolically active subcutaneous depot and brown fat. In our study, t-AUCB treatment dose-dependently reduce cholesterol content in epididymal fat of mice, which is consistent with the effect on cholesterol efflux. Our results support other studies that mice with targeted deletion or pharmacological inhibition of sEH prevented body weight gain, and reduced subcutaneous and visceral fat in high-fat induced obesity mice [21,34], although we observe no significant effect on body weight.

sEH gene polymorphism is associated with plasma lipid and lipoprotein level [35]. The present data demonstrate that inhibition of sEH is capable of reducing plasma LDL-C and increasing circulating HDL-C levels. Recently, Chung et al. [13] showed that lack of adipose ABCA1 impaired cholesterol efflux to apoA-I and reduced circulating HDL-C. We speculate that the observed decrease in plasma HDL-C is attributed to a role for t-AUCB in adipose ABCA1 expression. Studies in animal models have shown that raising circulating HDL by overexpression of apoA-I or infusion of recombinant HDL retards plaque development [3,4], thus, we chose to test the effects of t-AUCB on atherosclerosis. Atherosclerosis was first established in Ldlr$^{-/-}$ mice by feeding them ATD for 14 weeks. In this setting, treatment with t-AUCB for 4 weeks caused a dose-dependent reduction in lesion size. Our results agree with those of previous studies in which a sEHI (AEPU or AR9276) reduced the development of atherosclerosis in apoE$^{-/-}$ mice [17,18]. However, the precise mechanism of action was not demonstrated. HDL plays a key role in RCT by promoting cholesterol efflux from peripheral cells, and delivering acquired cholesterol to liver for excretion, a process that is believed to be atheroprotective [1]. To test the functionality of HDL generated in the setting of t-AUCB treatment, we performed an *in vivo* RCT assay that measures the integrated rate of movement of ^{3}H-cholesterol from macrophages to the serum, liver, bile and feces. t-AUCB showed a concentration dependent increase trend toward plasma ^{3}H-levels. *In vivo*, t-AUCB increased the amount of ^{3}H-cholesterol in the liver, bile and feces in a dose dependent manner, indicating stimulation of RCT. However, the smallest increase was observed in the liver. RCT is a dynamic process and different intermediate compartments may influence liver ^{3}H-counts from cholesterol in opposite directions; for example, improved adipocyte cholesterol efflux increases liver ^{3}H-levels, whereas enhanced flux through the liver to feces may decrease them [24,36]. Thus, we speculate that the excess cholesterol present in the plasma after the drug treatment could have already been transported through the liver to the bile and feces. This is consistent with our finding that treatment with t-AUCB increased not only the flux of ^{3}H-cholesterol into the liver but also the transport of ^{3}H-cholesterol out of the liver into bile, resulting in no net increase in hepatic ^{3}H-cholesterol at 48 h. Notably, this increase in RCT may reflect the actions of t-AUCB that its ability to increase HDL-C in plasma due to promote the efflux of cholesterol from adipose tissue by increasing expression of ABCA1. While it is not known whether t-AUCB is directly delivered to the arterial wall or taken up by circulating monocytes and delivered to plaques. Therefore, the reversal in the development of atherosclerosis by t-AUCB is associated with the promotion of RCT process.

Hyperlipidemia plays a causal role in progression of atherosclerosis [37]. Atherosclerotic lesions start with increased delivery and oxidation of LDL-C in the intima layer of the arterial wall that initiates LDL uptake by monocytes and macrophages to form foam cells [38]. In addition, LDL tends to destabilize platelet membrane activity and disrupt normal functions of macrophages and endothelium [39]. An important mechanism by which statins prevent atherosclerosis and exert therapeutic effects in coronary artery disease is by lowering LDL [39]. Consistent with our study, Zhang et al. [17] also demonstrated that sEH inhibition lowered circulating LDL, which could contribute, at least partially, to the attenuation of atherosclerosis.

5. Conclusion

Our study in Ldlr$^{-/-}$ mice shows that t-AUCB inhibits sEH activity and increases ABCA1 expression in adipose tissue, increases circulating HDL, enhances the RCT pathway, reduces LDL-C levels, and regresses established atherosclerosis. Put together, our results indicate that sEH might be a promising target for raising HDL in the treatment of cardiovascular disease.

Supplementary Material

Refer to Web version on PubMed Central for supplementary material.

Acknowledgments

Abbreviations

ABCA1	ATP binding cassette transporter A1
HDL	high-density lipoprotein
RCT	reverse cholesterol transport
sEH	soluble epoxide hydrolase
EETs	epoxyeicosatrienoic acids
DHETs	dihydroxyeicosatrienoic acids
sEHI	sEH inhibitors
ATD	atherogenic diet
t-AUCB	$trans$-4-[4-(3-adamantan-1-yl-ureido)-cyclohexyloxy]-benzoic acid
SCD	standard chow diet
acLDL	acetylated LDL

LSC liquid scintillation counting

References

1. McGillicuddy FC, Reilly MP, Rader DJ. Adipose modulation of high-density lipoprotein cholesterol: implications for obesity, high-density lipoprotein metabolism, and cardiovascular disease. Circulation. 2011; 124:1602–1605. [PubMed: 21986773]

2. Choudhury RP, Rong JX, Trogan E, et al. High-density lipoproteins retard the progression of atherosclerosis and favorably remodel lesions without suppressing indices of inflammation or oxidation. Arterioscler. Thromb. Vasc. Biol. 2004; 24:1904–1909. [PubMed: 15319266]

3. Plump AS, Scott CJ, Breslow JL. Human apolipoprotein A-I gene expression increases high density lipoprotein and suppresses atherosclerosis in the apolipoprotein E-deficient mouse. Proc. Natl. Acad. Sci. U. S. A. 1994; 91:9607–9611. [PubMed: 7937814]

4. Shah PK, Yano J, Reyes O, et al. High-dose recombinant apolipoprotein AI(milano) mobilizes tissue cholesterol and rapidly reduces plaque lipid and macrophage content in apolipoprotein e-deficient mice. Potential implications for acute plaque stabilization. Circulation. 2001; 103:3047–3050. [PubMed: 11425766]

5. Nissen SE, Tsunoda T, Tuzcu EM, et al. Effect of recombinant ApoA-I Milano on coronary atherosclerosis in patients with acute coronary syndromes: a randomized controlled trial. JAMA. 2003; 290:2292–2300. [PubMed: 14600188]

6. Yancey PG, Bortnick AE, Kellner-Weibel G, et al. Importance of different pathways of cellular cholesterol efflux. Arterioscler. Thromb. Vasc. Biol. 2003; 23:712–719. [PubMed: 12615688]

7. Young SG, Fielding CJ. The ABCs of cholesterol efflux. Nat. Genet. (1999; 22:316–318. [PubMed: 10431227]

8. Wellington CL, Walker EK, Suarez A, et al. ABCA1 mRNA and protein distribution patterns predict multiple different roles and levels of regulation. Lab. Investig. 2002; 82:273–283. [PubMed: 11896206]

9. Timmins JM, Lee JY, Boudyguina E, et al. Targeted inactivation of hepatic Abca1 causes profound hypoalphalipoproteinemia and kidney hypercatabolism of apoA-I. J. Clin. Invest. 2005; 115:1333–1342. [PubMed: 15841208]

10. Brunham LR, Kruit JK, Iqbal J, et al. Intestinal ABCA1 directly contributes to HDL biogenesis in vivo. J. Clin. Investig. 2006; 116:1052–1062. [PubMed: 16543947]

11. Krause BR, Hartman AD. Adipose tissue and cholesterol metabolism. J. Lipid Res. 1984; 25:97–110. [PubMed: 6368715]

12. Zhang Y, McGillicuddy FC, Hinkle CC, et al. Adipocyte modulation of high-density lipoprotein cholesterol. Circulation. 2010; 121:1347–1355. [PubMed: 20212278]

13. Chung S, Sawyer JK, Gebre AK, et al. Adipose tissue ATP binding cassette transporter A1 contributes to high-density lipoprotein biogenesis in vivo. Circulation. 2011; 124:1663–1672. [PubMed: 21931081]

14. Yvan-Charvet L, Ranalletta M, Wang N, et al. Combined deficiency of ABCA1 and ABCG1 promotes foam cell accumulation and accelerates atherosclerosis in mice. J. Clin. Investig. 2007; 117:3900–3908. [PubMed: 17992262]

15. De Taeye BM, Morisseau C, Coyle J, et al. Expression and regulation of soluble epoxide hydrolase in adipose tissue. Obesity (Silver Spring). 2010; 18:489–498. [PubMed: 19644452]

16. Shen L, Peng H, Zhao S, et al. A potent soluble epoxide hydrolase inhibitor, t-AUCB, modulates cholesterol balance and oxidized low density lipoprotein metabolism in adipocytes in vitro. Biol. Chem. 2014; 395:443–451. [PubMed: 24225128]

17. Zhang LN, Vincelette J, Cheng Y, et al. Inhibition of soluble epoxide hydrolase attenuated atherosclerosis, abdominal aortic aneurysm formation, and dyslipidemia. Arterioscler. Thromb. Vasc. Biol. 2009; 29:1265–1270. [PubMed: 19667112]

18. Ulu A, Davis BB, Tsai HJ, et al. Soluble epoxide hydrolase inhibitors reduce the development of atherosclerosis in apolipoprotein e-knockout mouse model. J. Cardiovasc. Pharmacol. 2008; 52:314–323. [PubMed: 18791465]

19. Hwang SH, Tsai HJ, Liu JY, et al. Orally bioavailable potent soluble epoxide hydrolase inhibitors. J. Med. Chem. 2007; 50:3825–3840. [PubMed: 17616115]

20. Li N, Liu JY, Timofeyev V, et al. Beneficial effects of soluble epoxide hydrolase inhibitors in myocardial infarction model: insight gained using metabolomic approaches. J. Mol. Cell. Cardiol. 2009; 47:835–845. [PubMed: 19716829]

21. Liu Y, Dang H, Li D, et al. Inhibition of soluble epoxide hydrolase attenuates high-fat-diet-induced hepatic steatosis by reduced systemic inflammatory status in mice. PLoS One. 2012; 7:e39165. [PubMed: 22720061]

22. Wolf NM, Morisseau C, Jones PD, et al. Development of a high-throughput screen for soluble epoxide hydrolase inhibition. Anal. Biochem. 2006; 355:71–80. [PubMed: 16729954]

23. Rayner KJ, Suarez Y, Davalos A, et al. MiR-33 contributes to the regulation of cholesterol homeostasis. Science. 2010; 328:1570–1573. [PubMed: 20466885]

24. McGillicuddy FC, de la Llera Moya M, Hinkle CC, et al. Inflammation impairs reverse cholesterol transport in vivo. Circulation. 2009; 119:1135–1145. [PubMed: 19221221]

25. Zhang Y, Zanotti I, Reilly MP, et al. Overexpression of apolipoprotein A-I promotes reverse transport of cholesterol from macrophages to feces in vivo. Circulation. 2003; 108:661–663. [PubMed: 12900335]

26. Spector AA, Norris AW. Action of epoxyeicosatrienoic acids on cellular function. Am. J. Physiol. Cell. Physiol. 2007; 292:C996eC1012. [PubMed: 16987999]

27. Newman JW, Morisseau C, Hammock BD. Epoxide hydrolases: their roles and interactions with lipid metabolism. Prog. Lipid Res. 2005; 44:1–51. [PubMed: 15748653]

28. Luo P, Chang HH, Zhou Y, et al. Inhibition or deletion of soluble epoxide hydrolase prevents hyperglycemia, promotes insulin secretion, and reduces islet apoptosis. J. Pharmacol. Exp. Ther. 2010; 334:430–438. [PubMed: 20439437]

29. Shen HC, Hammock BD. Discovery of inhibitors of soluble epoxide hydro-lase: a target with multiple potential therapeutic indications. J. Med. Chem. 2012; 55:1789–1808. [PubMed: 22168898]

30. Bettaieb A, Nagata N, AbouBechara D, et al. Soluble epoxide hydrolase deficiency or inhibition attenuates diet-induced endoplasmic reticulum stress in liver and adipose tissue. J. Biol. Chem. 2013; 288:14189–14199. [PubMed: 23576437]

31. Singaraja RR, Brunham LR, Visscher H, et al. Efflux and atherosclerosis: the clinical and biochemical impact of variations in the ABCA1 gene. Arterioscler. Thromb. Vasc. Biol. 2003; 23:1322–1332. [PubMed: 12763760]

32. Karasinska JM, Rinninger F, Lutjohann D, et al. Specific loss of brain ABCA1 increases brain cholesterol uptake and influences neuronal structure and function. J. Neurosci. 2009; 29:3579–3589. [PubMed: 19295162]

33. Rosen ED, Spiegelman BM. Adipocytes as regulators of energy balance and glucose homeostasis. Nature. 2006; 444:847–853. [PubMed: 17167472]

34. Sodhi K, Inoue K, Gotlinger KH, et al. Epoxyeicosatrienoic acid agonist rescues the metabolic syndrome phenotype of HO-2-null mice. J. Pharmacol. Exp. Ther. 2009; 331:906–916. [PubMed: 19717790]

35. Sato K, Emi M, Ezura Y, et al. Soluble epoxide hydrolase variant (Glu287Arg) modifies plasma total cholesterol and triglyceride phenotype in familial hypercholesterolemia: intrafamilial association study in an eight-generation hyperlipidemic kindred. J. Hum. Genet. 2004; 49:29–34. [PubMed: 14673705]

36. Malik P, Berisha SZ, Santore J, et al. Zymosan-mediated inflammation impairs in vivo reverse cholesterol transport. J. Lipid Res. 2011; 52:951–957. [PubMed: 21335620]

37. Teramoto T, Sasaki J, Ueshima H, et al. Goals of dyslipidemia management. J. Atheroscler. Thromb. 2007; 14:209–212. [PubMed: 17986796]

38. Shen L, Peng HC, Nees SN, et al. Proprotein convertase subtilisin/kexin type 9 potentially influences cholesterol uptake in macrophages and reverse cholesterol transport. FEBS Lett. 2013; 587:1271–1274. [PubMed: 23499248]

39. Vaughan CJ, Gotto AM Jr, Basson CT. The evolving role of statins in the management of atherosclerosis. J. Am. Coll. Cardiol. 2000; 35:1–10. [PubMed: 10636252]
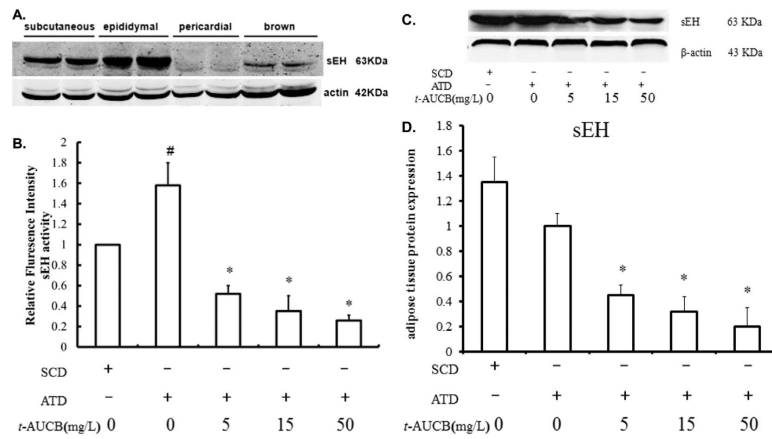
Fig. 1.

The activity and protein expression of sEH in adipose tissues. (**A**) The protein expression of sEH in epididymal, pericardial, inguinal (subcutaneous) and brown fat depot. (**B**) Epididymal adipose tissue was homogenized. Cytosolic supernatants were incubated with or without 20 μM *t*-AUCB in 96-well black assay plates. Fluorescence was determined by use of a Spectra Fluor Plus Xuorescent plate reader. sEH activity was the corrected sample fluorescence intensity calculated by sample fluorescence values for the sEHI subtracted from those of the non-sEHI. Data are presented as mean ± SD. (**C**) Western blot analysis of protein levels of sEH and β-actin in adipose tissue. (**D**) Analysis of the relative protein levels of sEH and β-actin as a normalization control in adipose tissue. *P < 0.05, compared to *t*-AUCB 0 mg/L group.
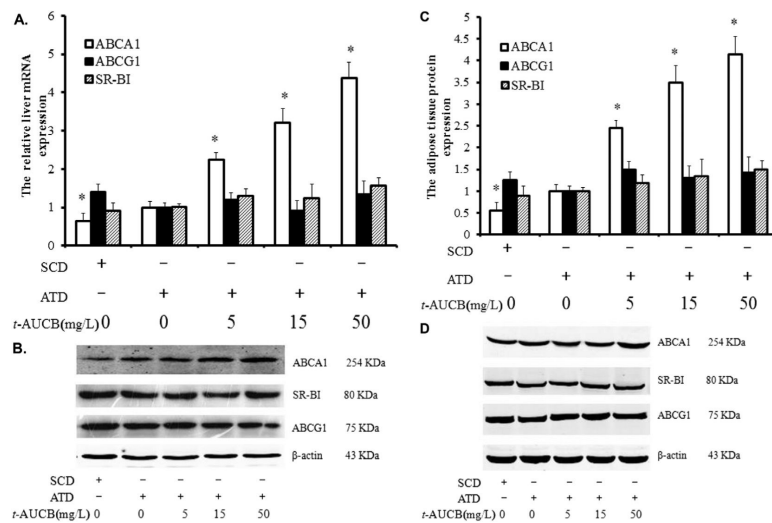
Fig. 2.

The expression of ABCA1, ABCG1 and SR-BI in epididymal adipose tissue and liver. (**A**) Reverse transcription polymerase chain reaction quantification of relative mRNA expression in liver of mice. The signal of *t*-AUCB 0 mg/L mice was set at a normalized value. GAPDH was used as internal control. (**B**) Western blot analysis of protein levels of ABCA1, ABCG1 and SR-BI in epididymal adipose tissue and (**C**) relative protein content compared to that of β-actin. (**D**) Western blot analysis of protein levels of ABCA1, ABCG1, SR-BI and β-actin as a normalization control in liver. Data are presented as mean ± SD. *$P < 0.05$, compared to *t*-AUCB 0 mg/L group.
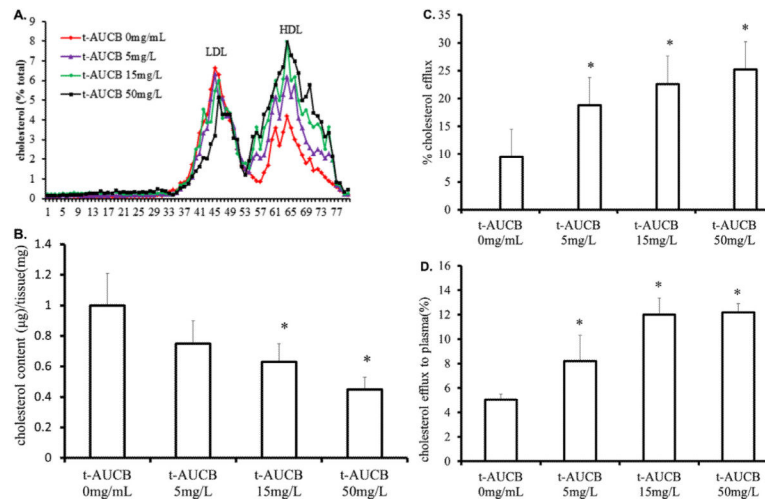
Figure 3.
The effect of *t*-AUCB on HDL levels and cholesterol efflux. (**A**) FPLC lipoprotein profiles from pooled plasma (n = 4) of *t*-AUCB-treated mice. (**B**) Cholesterol contents in epididymal adipose tissue. (**C**) *In vitro* cultures of epididymal fat from wide type and *t*-AUCB-treated mice were radiolabeled with ^{3}H-cholesterol for 24 h, washed, and then incubated with apoA-I (20 μg/mL) for 4 h to measure ^{3}H-cholesterol efflux into the medium. (**D**) *In vitro* cultures of 3T3-L1 adipocytes were radiolabeled with ^{3}H-cholesterol for 24 h, washed, and then incubated with plasma from wide type and *t*-AUCB-treated mice for 4 h to measure ^{3}H-cholesterol efflux into the medium. *$P < 0.05$, compared to *t*-AUCB 0 mg/L group.
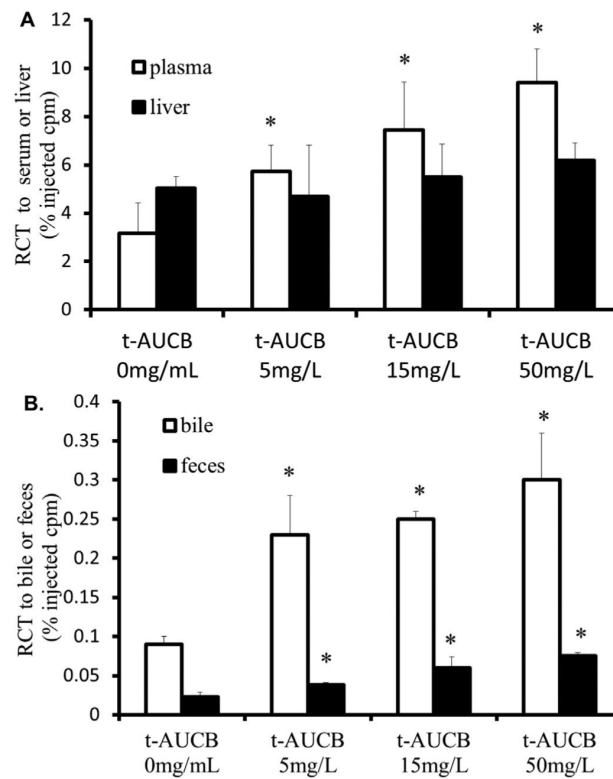
Fig. 4.
The effect of *t*-AUCB on RCT. The rate of RCT is increased in *t*-AUCB-treated mice. After 4 weeks of the indicated treatment, Ldlr$^{-/-}$ mice (n = 8/group) were injected intraperitoneally with ^{3}H-cholesterol-labeled, acLDL-loaded macrophages. Data are expressed as the percentage of the ^{3}H-cholesterol tracer relative to that of total cpm tracer injected ± SD. (**A**) ^{3}H-cholesterol distribution in plasma and liver after 48 h. (**B**) ^{3}H-cholesterol tracer levels in bile acid and feces. Feces were collected continuously from 0 to 48 h after injection. *$P < 0.05$, compared with *t*-AUCB 0 mg/mL.
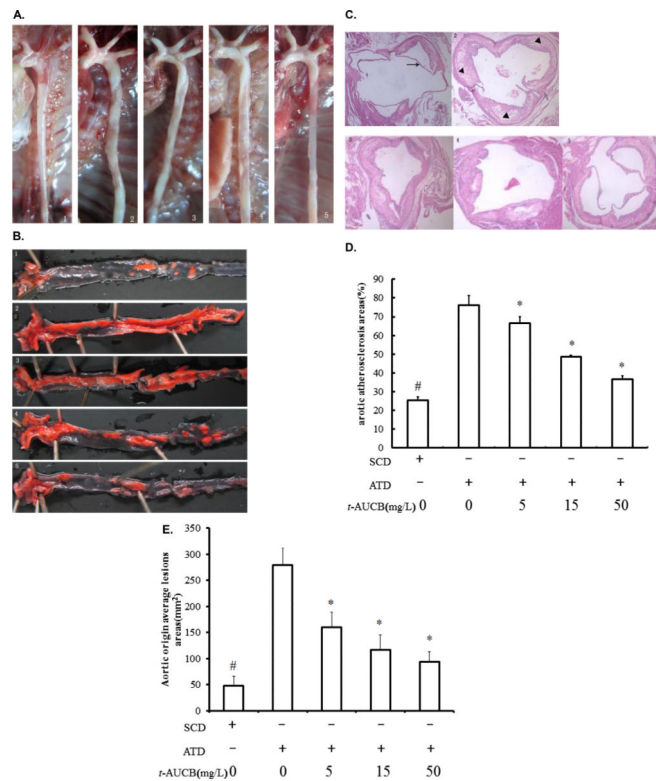
Fig. 5.
t-AUCB decreases plaque formation in Ldlr$^{-/-}$ mice. (**A**) Photographs of the gross appearance of atherosclerotic lesions in SCD and *t*-AUCB-fed mice were visualized in situ prior to staining, in which yellowish-white lesions are observed (1, SCD mice; 2, 3, 4, 5 represent ATD mice with 0, 5, 15, 50 mg/L *t*-AUCB treatment respectively). (**B**) Representative descending aorta of mice shown en face after staining with Sudan **III**. (**C**) Cross-section through the aortic sinus of mice stained with hematoxylin/eosin. The three valve leaflets (at arrow-heads) were filled with extensive lesions, which are showed at arrow. (**D**) Quantitative measurement of data in **B** from all mice. The extent of covered lesions in entire aorta is shown as a percentage of the surface area. (**E**) Quantitative measurement of data in **C** from mice. The average lesion size in cross-sections through the aortic origin is indicated in μm^2. Values are mean ± SEM. Control group *n* = 6, *t*-AUCB treated group *n* = 32. Data represent mean ± S.D. $^{\#}P < 0.05$, compared to SCD group, $*P < 0.05$, compared to *t*-AUCB 0 mg/L group (magnification: ×20).

Table 1

The effect of *t*-AUCB on plasma lipid levels and body weight. Body weight was obtained at baseline (after 14 weeks ATD) and at sacrifice (after 4 weeks treatment with *t*-AUCB 0, 5,15, 50 mg/mL). Total plasma TC, LDL-C and HDL-C levels were obtained at sacrifice. All data are expressed as mean ± SD (n = 8 mice/group).

	SCD	Baseline	*t*-AUCB 0 mg/mL	*t*-AUCB 5 mg/mL	*t*-AUCB 15 mg/mL	*t*-AUCB 50 mg/mL
Starting treatment BW (g)	21.8 ± 1.93	29.4 ± 2.5[#]	30.8 ± 3.5	31.2 ± 2.8	28.9 ± 3.1	30.4 ± 2.4
BW at sacrifice (g)	22.6 ± 2.4	30.5 ± 1.8[#]	31.5 ± 2.5	29.8 ± 2.2	29.0 ± 2.3	28.5 ± 3.3
TG (mmol/L)	1.22 ± 0.21	1.48 ± 0.28	1.36 ± 0.32	1.13 ± 0.19	1.19 ± 0.12	1.09 ± 0.09
TC (mmol/L)	11.56 ± 2.6	24.8 ± 1.1[#]	23.3 ± 1.4	24.6 ± 1.2	22.5 ± 1.9	21.4 ± 1.5
LDL-C (mmol/L)	7.63 ± 1.6	14.3 ± 1.9[#]	14.4 ± 1.3	10.4 ± 2.1[*]	9.6 ± 2.9[*]	8.9 ± 1.9[*]
HDL-C (mmol/L)	1.43 ± 0.28	0.76 ± 0.1[#]	0.71 ± 0.26	1.0 ± 0.06[*]	1.2 ± 0.1[*]	1.4 ± 0.15[*]
NEFAs (mg/dl)	0.68 ± 0.11	0.79 ± 0.16	0.62 ± 0.06	0.69 ± 0.12	0.88 ± 0.15	0.73 ± 0.18

[#]P < 0.05, SCD vs baseline

[*]P < 0.05, *t*-AUCB 0 mg/L vs 5, 15, 50 mg/L groups.